Macromolecules

ARTICLE

pubs.acs.org/Macromolecules

Polyaniline Nanorings and Flat Hollow Capsules Synthesized by *in Situ* Sacrificial Oxidative Templates

Guicun Li,* Yingmei Li, Yan Li, Hongrui Peng, and Kezheng Chen*

Laboratory of Functional and Biological Nanomaterials, College of Materials Science and Engineering, Qingdao University of Science and Technology, Qingdao 266042, P.R. China

Supporting Information

ABSTRACT: An *in situ* sacrificial oxidative template route has been developed for the bulk synthesis of two-dimensional polyaniline nanostructures, such as nanorings and flat hollow capsules. In the reaction system, $VOPO_4 \cdot 2H_2O$ nanoplates formed spontaneously in $V_2O_5/H_2O_2/H_3PO_4$ mixture can serve as both oxidant and sacrificial template for the chemical oxidative polymerization of aniline. The synthetic parameters, such as reaction times, the concentrations of H_3PO_4, and types of the oxidants on the morphologies, sizes, and molecular structures of polyaniline nanostructures have been investigated. The time-dependent experiments reveal that $VOPO_4 \cdot 2H_2O$ nanoplate is etched gradually with the polymerization reaction proceeding. The concentration of H_3PO_4 can adjust the polymerization rate of aniline as well as the etching rate of $VOPO_4 \cdot 2H_2O$, which is critical for controlled synthesis of polyaniline nanorings and flat hollow capsules. The sacrificial oxidative template approach can be extended to synthesize two-dimensional polypyrrole nanostructures.

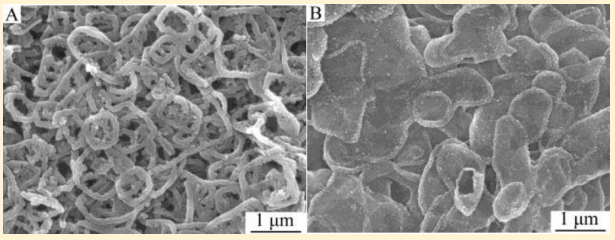

INTRODUCTION

During the past few decades, intrinsically conducting polymers have attracted great interest due to their fascinating electrical, optical, and electrochemical properties derived from the conjugated π-electron system.[1] Polyaniline is unique among the conducting polymers because of its simple synthesis, environmental stability, and reversible acid−base doping−dedoping process.[1−3] The conventional chemical oxidative polymerization of aniline in dilute aqueous acids using ammonium peroxydisulfate oxidant yields irregular granular aggregates and a small portion of nanofibers. The poor processability of polyaniline granular aggregate remains a key hurdle to its practical applications in various fields.

In recent years, polyaniline micro/nanostructures, such as nanoparticles, nanofibers, nanorods, nanobelts, nanotubes, nanoplates, nanoclips, and hollow spheres (capsules), have drawn considerable attention because of their improved solution processability, physical and chemical properties differing from their bulk counterpart, and great potential for a variety of applications including chemical sensors,[4,5] biosensors,[6] actuators,[7] superhydrophobic and superhydrophilic devices,[8,9] and molecular memory devices.[10] The high interfacial area in combination with electrochemical activity have endowed polyaniline with enhanced performances in various fields. A number of synthetic routes, including the use of templates[11−15] or surfactants,[16−20] interfacial polymerization,[21,22] oligomer-assisted polymerization,[23,24] rapidly mixed reaction,[25−27] seeding polymerization,[28] falling pH polymerization,[29−33] and dilute polymerization,[34] have been developed to synthesize polyaniline micro/nanostructures. Although ammonium peroxydisulfate is the most widely used oxidant, other oxidants, such as $FeCl_3$,[35] vanadium oxide,[26,36] and MnO_2,[12,13] can also be employed for the chemical oxidative polymerization of aniline for adjusting the sizes, morphologies, and molecular structures of polyaniline micro/nanostructures. Although a variety of synthetic methods have been reported for one-dimensional polyaniline nanostructures, the controlled synthesis of two-dimensional (2D) polyaniline nanostructures using a facile effective method still remains scientifically challenging. Herein, we report an *in situ* sacrificial oxidative template route to synthesize bulk quantity of 2D polyaniline nanostructures including nanorings and flat hollow capsules.

EXPERIMENTAL SECTION

Synthesis of Polyaniline Nanorings. In a typical synthesis, 0.18 g of commercial orthorhombic V_2O_5 powder was dissolved into 2 mL of 30% H_2O_2 solution. After a highly exothermic reaction, 10 mL of 1 mol/L H_3PO_4 aqueous solution was added with stirring to form a yellow slurry. Then 5 mL of 0.2 mol/L aniline aqueous solution was rapidly transferred to the above mixture. The polymerization reaction was carried out for 12 h at room temperature. The dark green precipitate was filtered off, washed with deionized and ethanol several times, and dried at room temperature for 24 h

Characterization. The morphologies and sizes of polyaniline samples were characterized by field-emission scanning electron microscopy (FE-SEM, JSM 6700) and transmission electron microcopy (TEM, JEM 2000EX). Samples for SEM were deposited onto Si wafer

Received: June 29, 2011
Revised: September 28, 2011
Published: November 03, 2011

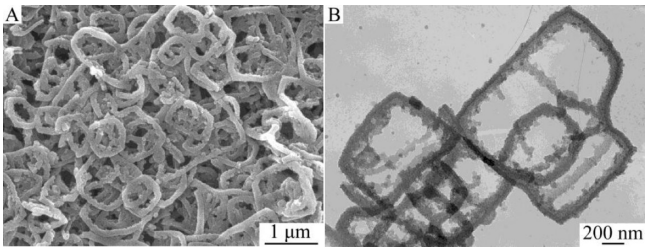

Figure 1. SEM (A) and TEM (B) images of polyaniline nanorings.

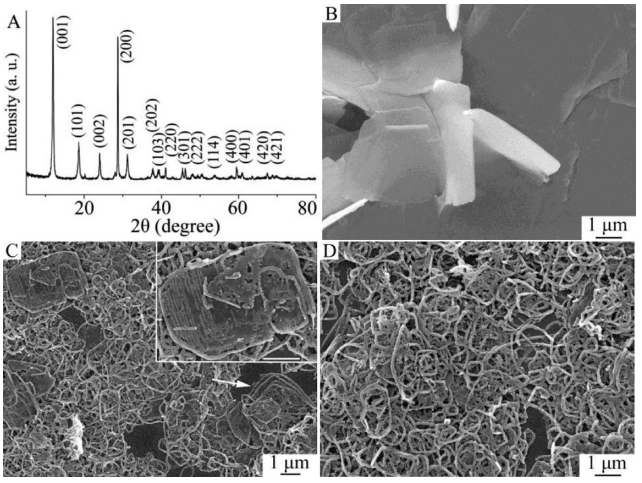

Figure 2. XRD pattern (A) and SEM image (B) of $VOPO_4 \cdot 2H_2O$ nanoplates; SEM image of the intermediate products synthesized for 0.5 (C) and 1 h (D). The inset in part C shows the corresponding high-magnification SEM image and the scale bar in the inset is 1 μm.

substrates and sputtered with a thin layer of Pd. Sample dispersed in deionized water are transferred to copper grids for TEM observation. The crystal structure of the oxidant formed before polymerization reaction was analyzed by powder X-ray diffraction (XRD, Rigaku D-max-γA XRD Cu Kα radiation, λ = 1.54178 Å). The molecular structures of polyaniline samples were measured by Fourier transform infrared (FTIR, Nicolet Magna IR-750 spectrophotometer) spectroscopy using KBr pressed disks, and UV−vis spectroscopy (Cary 500 UV−vis−NIR spectrophotometer) with the samples dispersed in deionized water. The conductivity of polyaniline samples is measured by the four point technique using a Jandel four point probe head. The samples are first compressed to 100 μm thick films and then measure the resistance. The cyclic voltammograms of polyaniline samples were determined in a 0.1 mol/L H_2SO_4 aqueous solution with a scan rate of 0.05 V/s using a CHI660C electrochemical workstation.

RESULTS AND DISCUSSION

Typical SEM and TEM images of polyaniline nanorings are shown in Figure 1A and B, respectively. Low-magnification SEM image (Figure S1, see Supporting Information) reveals that the polyaniline sample consists of a large quantity of ring-like nanostructures with quasi-rectangular shapes (0.7 mol/L H_3PO_4). As shown in high-magnification SEM image (Figure 1A), it can be seen clearly that the nanorings are seamless. The diameters of the rings range from several hundred of nanometers to several micrometers, and the wall thickness is about 100 nm. The ring-like nanostructures of polyaniline can be further confirmed by

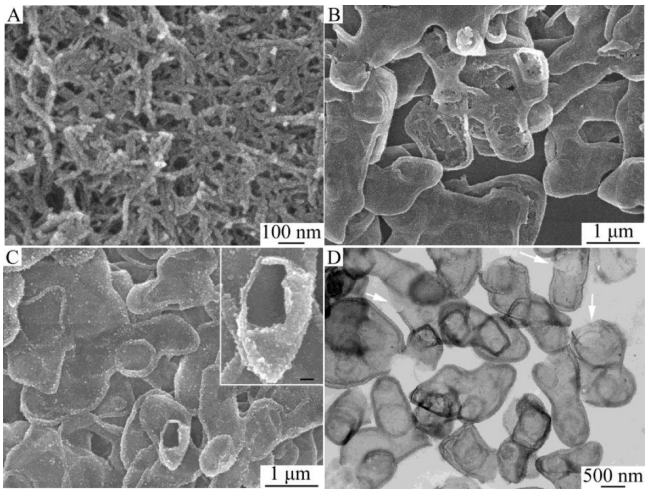

Figure 3. SEM (A−C) and TEM (D) images of polyaniline micro/nanostructures synthesized with different concentrations of H_3PO_4. Key: (A) 0.2 mol/L; (B) 1.8 mol/L; (C, D) 3.6 mol/L. The inset in part C showing a typical broken polyaniline hollow capsule, and the scale bar is 100 nm.

TEM image (Figure 1B). The sizes of polyaniline nanorings are similar to that in Figure 1A.

To investigate the formation process of polyaniline nanorings, time-dependent experiments were carried out at room temperature for different reaction times. Before polymerization reaction, V_2O_5 is dissolved in H_2O_2 solution to form peroxovanadic acid, which can react with H_3PO_4 (0.7 mol/L) to form insoluble yellow product. Figure 2A shows typical X-ray diffraction (XRD) pattern of the yellow product. All the diffraction peaks can be indexed to tetragonal crystalline phase $VOPO_4 \cdot 2H_2O$ with calculated lattice constants a = 6.212 Å and c = 7.414 Å, which is in agreement with literature values (JCPDS 361472). SEM image of the $VOPO_4 \cdot 2H_2O$ sample (Figure 2B) shows quasi-rectangular plate-like morphology with smooth surfaces. The lateral dimensions and thickness of $VOPO_4 \cdot 2H_2O$ nanoplates are about several micrometers and several tens of nanometers, respectively. The basic reaction for the formation of $VOPO_4 \cdot 2H_2O$ nanoplates can be described as follows: $V_2O_5 + 2H_2O_2 + 2H_3PO_4 \rightarrow 2VOPO_4 \cdot 2H_2O\downarrow + H_2O + O_2\uparrow$. When aniline was added into the $VOPO_4 \cdot 2H_2O$ slurry, the color of the mixture was changed from yellow to green, indicating the polymerization reaction of aniline can be initiated by $VOPO_4 \cdot 2H_2O$. As the polymerization reaction was performed for 0.5 h, besides polyaniline nanorings, some $VOPO_4 \cdot 2H_2O$ nanoplates remain in the intermediate product, which is encircled by polyaniline (Figure 2C and its inset). It is clear that the wall thickness of polyaniline nanorings is larger than the thickness of $VOPO_4 \cdot 2H_2O$ nanoplates. Moreover, some concentric polyaniline nanorings can also be found in the intermediate product as indicated by an arrow, indicating that $VOPO_4 \cdot 2H_2O$ nanoplate acting as sacrificial oxidative templates is depleted gradually to initiate polymerization reaction of aniline to form concentric polyaniline nanorings with different diameters. After 1 h, it is clear that most of the $VOPO_4 \cdot 2H_2O$ templates are removed due to the subsequent polymerization reaction of aniline (Figure 2D).

The synthetic parameters, such as the concentrations of H_3PO_4, and types of the oxidants, have profound influences on the morphologies of polyaniline micro/nanostructures. Figure 3

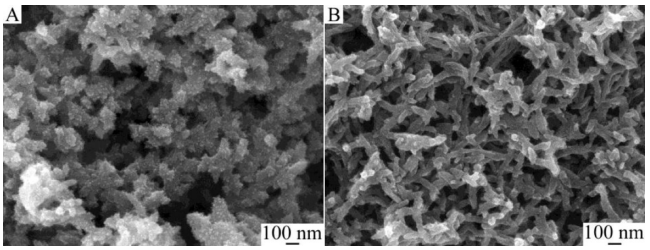

Figure 4. SEM images of polyaniline nanostructures synthesized with different concentrations of H_3PO_4 using ammonium peroxydisulfate as the oxidant. Key: (A) 0.7 mol/L; (B) 3.6 mol/L.

represents SEM and TEM images of polyaniline micro/nanostructures synthesized with different concentrations of H_3PO_4. As the concentration of H_3PO_4 is decreased to 0.2 mol/L, SEM image (Figure S2A, see Supporting Information) shows that the formed oxidant exists in the form of film, and no nanoplate is found. After polymerization, one can observe that the product is composed of polyaniline nanofibers with diameters of about 20 nm and lengths up to several hundred nanometers. As the concentration of H_3PO_4 is increased to 1.8 mol/L, there is a small portion of polyaniline nanorings in addition to plate-like polyaniline microstructures (Figure 3B). As shown in Figure 3C, higher H_3PO_4 concentration (3.6 mol/L) yields pure plate-like polyaniline microstructures with lateral dimensions of several micrometers, which is related to the plate-like $VOPO_4 \cdot 2H_2O$ oxidant (Figure S2B, see Supporting Information). A typical hole in a broken polyaniline microstructure (the inset in Figure 3C) indicates that the plate-like polyaniline microstructures have hollow interior, which is highly reminiscent of deflated balloons or flat hollow capsules, and distinct from polyaniline hollow microspheres reported previously.[12−14,18] The wall thickness of polyaniline flat hollow capsules is about 20 nm. Typical TEM image of polyaniline flat hollow capsules is shown in Figure 3D. The strong contrast between the dark edge and pale center demonstrates the hollow structures of polyaniline, revealing that the residual $VOPO_4 \cdot 2H_2O$ have been etched completely with the polymerization reaction proceeding. The walls can be seen clearly in some broken hollow capsules as indicated by arrows. For comparison purposes, ammonium peroxydisulfate is used to replace V_2O_5 in the reaction system. When the concentrations of H_3PO_4 are 0.7 and 3.6 mol/L, coral-like polyaniline nanostructures (Figure 4A) and netlike polyaniline nanofibers (Figure 4B) are obtained, respectively. On the basis of the experimental results (Figures 1−3), it is clear that $VOPO_4 \cdot 2H_2O$ nanoplates can serve as sacrificial oxidative templates for the formation of polyaniline nanorings and flat hollow capsules. Before aniline is added, $VOPO_4 \cdot 2H_2O$ nanoplates are formed first. Once the polymerization reaction of aniline occurs, $VOPO_4 \cdot 2H_2O$ nanoplates will be reduced and etched gradually by H_3PO_4 and the 2D morphologies of $VOPO_4 \cdot 2H_2O$ are replicated by polyaniline. The concentration of H_3PO_4 can adjust the polymerization rate of aniline as well as the etching rate of $VOPO_4 \cdot 2H_2O$, which is critical for controlled synthesis of 2D polyaniline nanostructures. At low H_3PO_4 concentration (0.7 mol/L H_3PO_4), the polymerization of aniline is slow and occurs preferentially on the edges of $VOPO_4 \cdot 2H_2O$ nanoplates to form polyaniline nanorings due to the higher surface energy and small size of the edges. However, high H_3PO_4 concentration (3.6 mol/L H_3PO_4) increases the polymerization rate of anilne, so polymerization reaction happens

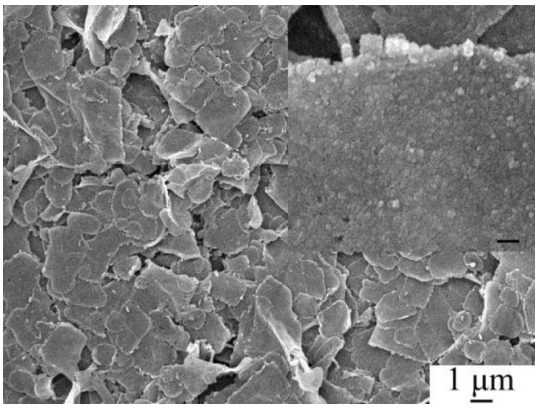

Figure 5. SEM images of polypyrrole nanoplates synthesized with 0.7 mol/L H_3PO_4 using $VOPO_4 \cdot 2H_2O$ nanoplates as sacrificial oxidative templates. The inset shows a high-magnification SEM image of polypyrrole nanoplates, and the scale bar is 100 nm.

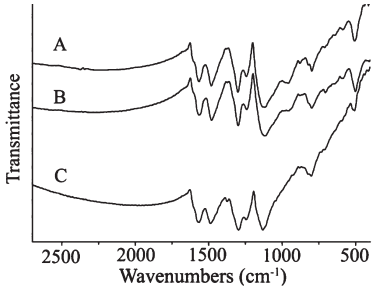

Figure 6. FTIR spectra of polyaniline micro/nanostructures. Key: (A) polyaniline nanorings (Figure 1); (B) polyaniline hollow capsules (Figure 3C and D); (C) polyaniline nanofibers (Figure 4B).

on all the surfaces of $VOPO_4 \cdot 2H_2O$ nanoplates, yielding polyaniline flat hollow capsules. The $VOPO_4 \cdot 2H_2O$ oxidative template route can be extended to synthesize polypyrrole nanostructures (Figure 5). As shown in Figure 5, the product is composed of a large quantity of polypyrrole nanoplates with lateral dimensions of several nanometers. High-magnification SEM image (the inset in Figure 5) shows that the polypyrrole nanoplates composed of nanoparticles have solid structures and are about 35 nm in thickness, which is different from polyaniline. However, the shapes of $VOPO_4 \cdot 2H_2O$ oxidative templates are still preserved, demonstrating the $VOPO_4 \cdot 2H_2O$ nanoplates act as oxidative templates for the polymerization reaction of aniline or pyrrole.

The molecular structures of polyaniline nanorings and flat hollow capsules were characterized by FTIR and UV−vis−NIR spectroscopies. FTIR spectra of polyaniline nanorings (Figure 1), hollow capsules (Figure 3, parts C and D), and nanofibers (Figure 4B) are presented in Figure 6. For polyaniline nanorings and hollow capsules, the bands at around 1565, 1481, 1300, 1243, and 1118 cm^{-1} can be ascribed to C═C stretching in the quinoid rings, C═C stretching in the benzenoid rings, C−N stretching vibration of the secondary aromatic amine, the protonated C−N group, and aromatic C−H in-plane bending, respectively. For polyaniline nanofibers, the corresponding bands are located at 1565, 1487, 1295, 1244, and 1132 cm^{-1}, respectively.[17−19] It is indicated that the molecular structures of polyaniline are not changed greatly by the H_3PO_4 concentration (Figure S3, see Supporting Information), and

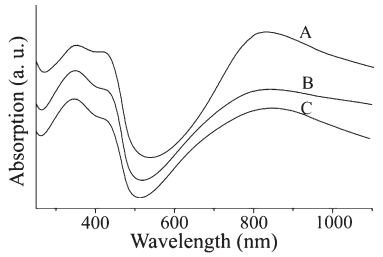

Figure 7. UV−vis−NIR spectra of polyaniline micro/nanostructures. Key: (A) polyaniline nanorings (Figure 1); (B) polyaniline hollow capsules (Figure 3C and D); (C) polyaniline nanofibers (Figure 4B).

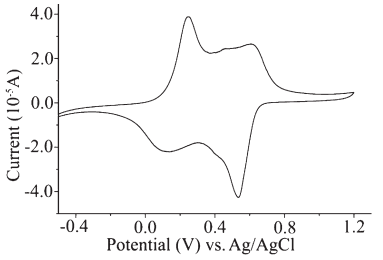

Figure 8. Cyclic voltammograms of polyaniline nanorings in 1 mol/L H_2SO_4 aqueous solution at a scan rate of 0.05 V/s.

the types of the oxidants. UV−vis-NIR spectra of polyaniline nanorings (Figure 1), hollow capsules (Figure 3, parts C and D), and nanofibers (Figure 4B) exhibit typical band characteristics of conventional polyaniline (Figure 7). The absorption bands at around 350, 430, and 850 nm can be attributed to $\pi \rightarrow \pi^*$ electronic transition, polaron band $\rightarrow \pi^*$ electronic transition, and the π to the localized polaron band, respectively.[21,22,34] A tail of the broad band at 850 nm extends into the NIR region, which is an indication of the emeraldine salt oxidation state of polyaniline.[34] The conductivities of polyaniline nanorings (Figure 1) and polyaniline nanofibers (Figure 4B) are 0.15 and 0.58 S/cm, respectively. The cyclic voltammograms of polyaniline nanorings (Figure 8) show two redox peak characteristic of the conventional polyaniline,[28] indicating that the aqueous electrochemistry of polyaniline is not affected significantly by $VOPO_4 \cdot 2H_2O$ oxidant.

CONCLUSIONS

In summary, we have developed an *in situ* sacrificial oxidative template route for the bulk synthesis of 2D polyaniline nanostructures including nanorings and flat hollow capsules for the first time. The $VOPO_4 \cdot 2H_2O$ nanoplates formed spontaneously in the $V_2O_5/H_2O_2/H_3PO_4$ system can serve as both the oxidant and template for the chemical oxidative polymerization of aniline, which can adjust the morphologies, sizes, and molecular structures of polyaniline. The morphological control of polyaniline nanostructures can be achieved easily by changing the synthetic parameters, e.g., the concentration of H_3PO_4. The sacrificial oxidative template approach can also be employed to the fabrication of polypyrrole nanostructures.

ASSOCIATED CONTENT

Supporting Information. Low-magnification SEM image of polyaniline nanorings, SEM images of $VOPO_4 \cdot 2H_2O$ templates synthesized with different concentrations of H_3PO_4, and FTIR spectrum of polyaniline nanofibers synthesized with 0.2 mol/L H_3PO_4.This material is available free of charge via the Internet at http://pubs.acs.org.

AUTHOR INFORMATION

Corresponding Author

*Telephone: 86-532-84022814. Fax: 86-532-84022814. E-mail: (G.L.) guicunli@qust.edu.cn; (K.C.) kchen@qust.edu.cn.

ACKNOWLEDGMENT

This work was supported by the Science and Technology Planning Project of Qingdao (10-3-4-4-8-jch), a Project of Shandong Province Higher Educational Science and Technology Program (J10LD02), and the Natural Science Foundation of Shandong Province (2009ZRB01034).

REFERENCES

(1) MacDiarmid, A. G. *Angew. Chem., Int. Ed.* **2001**, *40*, 2581.
(2) Huang, W. S.; Humphrey, B. D.; MacDiarmid, A. G. *J. Chem. Soc. Faraday Trans.* **1986**, *82*, 2385.
(3) MacDiarmid, A. G. *Synth. Met.* **1997**, *84*, 27.
(4) Virji, S.; Huang, J.; Kaner, R. B.; Weiller, B. H. *Nano Lett.* **2004**, *4*, 491.
(5) Janata, J.; Josowicz, M. *Nat. Mater.* **2003**, *2*, 19.
(6) Sangodkar, H.; Sukeerthi, S.; Srinivasa, R. S.; Lal, R.; Contractor, A. Q. *Anal. Chem.* **1996**, *68*, 779.
(7) Baker, C. O.; Shedd, B.; Innis, P. C.; Whitten, P. G.; Spinks, G. M.; Wallace, G. G.; Kaner, R. B. *Adv. Mater.* **2008**, *20*, 155.
(8) Chiou, N. R.; Lu, C.; Guan, J.; Lee, L. J.; Epstein, A. J. *Nat. Nanotech.* **2007**, *2*, 354.
(9) Zhu, Y.; Hu, D.; Wan, M.; Jiang, L.; Wei, Y. *Adv. Mater.* **2007**, *19*, 2092.
(10) Tseng, R. J.; Huang, J.; Ouyang, J.; Kaner, R. B.; Yang, Y. *Nano Lett.* **2005**, *5*, 1077.
(11) Wu, C. G.; Bein, T. *Science* **1994**, *264*, 1757.
(12) Pan, L.; Pu, L.; Shi, Y.; Song, S.; Xu, Z.; Zhang, R.; Zheng, Y. *Adv. Mater.* **2007**, *19*, 461.
(13) Fei, J.; Cui, Y.; Yan, X.; Yang, Y.; Wang, K.; Li, J. *ACS Nano* **2009**, *3*, 3714.
(14) Bai, M. Y.; Cheng, Y. J.; Wickline, S. A.; Xia, Y. *Small* **2009**, *5*, 1747.
(15) Zhang, Z.; Sui, J.; Zhang, L.; Wan, M. X.; Wei, Y.; Yu, L. *Adv. Mater.* **2005**, *17*, 2854.
(16) Liu, Z.; Zhang, X.; Poyraz, S.; Surwade, S. P.; Manohar, S. K. *J. Am. Chem. Soc.* **2010**, *132*, 13158.
(17) Wei, Z.; Zhang, L.; Yu, M.; Yang, Y.; Wan, M. *Adv. Mater.* **2003**, *15*, 1382.
(18) Wei, Z.; Wan, M. *Adv. Mater.* **2002**, *14*, 1314.
(19) Li, G.; Zhang, Z. *Macromolecules* **2004**, *37*, 2683.
(20) Zhang, C.; Li, G.; Peng, H. *Mater. Lett.* **2009**, *63*, 592.
(21) Huang, J.; Virji, S.; Weiller, B. H.; Kaner, R. B. *J. Am. Chem. Soc.* **2003**, *125*, 314.
(22) Huang, J.; Kaner, R. B. *J. Am. Chem. Soc.* **2004**, *126*, 851.
(23) Tran, H. D.; Wang, Y.; D'Arcy, J. M.; Kaner, R. B. *ACS Nano* **2008**, *2*, 1841.
(24) Surwade, S. P.; Manohar, N.; Manohar, S. K. *Macromolecules* **2009**, *42*, 1792.
(25) Huang, J.; Kaner, R. B. *Angew. Chem., Int. Ed.* **2004**, *43*, 5817.
(26) Li, G.; Jiang, L.; Peng, H. *Macromolecules* **2007**, *40*, 7890.
(27) Li, G.; Zhang, C.; Li, Y.; Peng, H.; Chen, K. *Polymer* **2010**, *51*, 1934.
(28) Zhang, X.; Goux, W. J.; Manohar, S. K. *J. Am. Chem. Soc.* **2004**, *126*, 4502.

(29) Stejskal, J.; Sapurina, I.; Trchová, M.; Konyushenko, E. N.; Holler, P. *Polymer* **2006**, *47*, 8253.
(30) Chiou, N. R.; Lee, L. J.; Epstein, A. J. *Chem. Mater.* **2007**, *19*, 3589.
(31) Li, G.; Zhang, C.; Peng, H. *Macromol. Rapid Commun.* **2008**, *29*, 63.
(32) Li, G.; Zhang, C.; Peng, H.; Chen, K.; Zhang, Z. *Macromol. Rapid Commun.* **2008**, *29*, 1954.
(33) Venancio, E. C.; Wang, P. C.; MacDiarmid, A. G. *Synth. Met.* **2006**, *156*, 357.
(34) Chiou, N. R.; Epstein, A. J. *Adv. Mater.* **2005**, *17*, 1679.
(35) Zhang, L.; Wan, M.; Wei, Y. *Macromol. Rapid Commun.* **2006**, *27*, 366.
(36) Pang, S.; Li, G.; Zhang, Z. *Macromol. Rapid Commun.* **2005**, *26*, 1262.